




New strategy for selective voltammetric determination of norepinephrine using modified electrode by using benzoyl ferrocene and manganese ferrite nanoparticles

Shayesteh Jafarei¹, Hamideh Asadollahzadeh^{1,*} , Nahid Rastakhiz¹, Mahdiah Ghazizadeh¹, and Sayed Zia Mohammadi²

¹Department of Chemistry, Faculty of Science, Kerman Branch, Islamic Azad University, Kerman, P. O. Box 7635131167, Iran

²Department of Chemistry, Payame Noor University, Tehran, Iran

Received: 11 November 2021

Accepted: 21 March 2022

Published online:
21 April 2022

© The Author(s), under exclusive licence to Springer Science+Business Media, LLC, part of Springer Nature 2022

ABSTRACT

Norepinephrine (NE) is one of the most important catecholamine neurotransmitters in the central nervous system and play an important role in health and diseases. Therefore, the determination of NE in biological samples is important for human health control purposes. In the present work, a new sensor has been constructed using a carbon paste electrode (CPE) modified by using benzoyl ferrocene and manganese ferrite nanoparticles (MF NPs) for norepinephrine determination. The hydrothermal method was used for synthesis of MF NPs. The synthesized NPs have been characterized by XRD pattern, scanning electron microscope (SEM), FT-IR, and EDX measurements. The obtained results illustrate that, the synthesized MF NPs have the spherical morphology with a mean diameter of 27.6 nm. The obtained data showed that the oxidation of NE at the surface of the modified CPE compared to bare CPE occurs at lower potentials and with higher current intensities. The oxidation peak current increased linearly with concentration over the two range of 0.03–10.0 μM and 10.0–500.0 μM with the detection limit of 20.0 nM. The reproducibility and stability of sensor were excellent and used successfully to detect of NE in blood serum and urine samples and high recoveries were obtained.

1 Introduction

Norepinephrine (NE) belongs to the class of catecholamine neurotransmitters, which plays pivotal role in the functioning of central nervous system [1, 2]. The behavioral and physiological conditions in

humans are controlled by neurotransmitters [3–5]. The neurotransmitters are involved in many neurobiological processes within the human body, such as memory, sleep, appetite and learning [3–5]. It is now well-established that defects in the secretion or absorption of neurotransmitters can lead to diseases

Address correspondence to E-mail: asadollahzadeh90@yahoo.com

such as Depression Syndrome, Neurological Diseases, and Drug Addiction [3–5].

One of the most important neurotransmitters is NE, which controls mood disorders, blood pressure, and emotional arousal. NE converts glycogen to glucose and also facilitates the conversion of fats into fatty acids, which in turn increases energy production. NE increases heart rate, opens the airways, and narrows blood vessels, therefore the human body can function well in stressful situations [3–5]. Analysis of published data from many laboratories involving more than 800 supine, resting, healthy subjects indicated an average circulating level of venous NE of 260 pg mL^{-1} [6]. According to the points mentioned above, knowing the concentration of NE in blood plasma is useful for diagnosing and evaluating the therapeutic and pharmacodynamic effects of psychiatric, neurological, and cardiovascular disorders.

A major problem in selectively determining NE is the presence of ascorbic acid (AA) and uric acid (UA) that are major interferents [7]. Therefore, the development of easy and sensitive methods that are also selective is crucial for the direct determination of NE.

Until now different analytical methods have been used for the determination of NE such as electrochemical techniques [7–17], gas chromatography [18], high performance liquid chromatography-mass spectrometry [19], ion chromatography with direct conductivity detection [20] and spectrophotometry [21]. Among the reported methods for measuring NE, the electrochemical technique has received more attention due to its advantages such as high sensitivity, high selectivity, ease and speed [7]. However, using unmodified electrodes, selective determination of NE in the presence of UA and AA is not possible because the oxidation potential of these substances is close to the oxidation potential of NE [7, 16].

The nanochemistry is applied in various areas of technology and science such as advanced materials, chemistry, optics, physics and biomedicine [22, 23]. Recently, with the development of new nanoparticles (NPs), the field of nanomedicine has expanded widely in the fields of diagnosis, monitoring and treatment of several diseases such as Parkinson, cancer and Alzheimer [24].

There are various methods of signal amplification with the aid of loading nanosphere, nanotube, nanosheet and nanoparticle on the electrode to fabricate electrochemical sensors [24–31]. The nanomaterials have excellent catalytic and electronic traits to

convert bio recognition processes into electrochemical reaction, and also have large surface area to increase the speed of electron exchange [16, 32–39].

Recently, metal oxide NPs have received more attention in different biological applications due to their diversity, stability and sensitivity [40]. Bimetallic NPs compared to monometallic NPs due to their magnetic, catalytic, optical and electrical properties have attracted more attention of researchers [41, 42].

In this research, a manganese ferrite nanoparticle (MF) was synthesized and then along with benzoyl ferrocene (BF) were used to modify the carbon paste electrode. The figure of merit of the BF-MF-modified carbon paste electrode (BFMFCPE) developed in the present work are the wider linear range [2, 3, 8, 11–14] and lower detection limit [2, 9, 11–14] compared to other reported electrodes for NE measurement.

Finally, the applicability of the modified electrode for measuring norepinephrine in human urine and serum samples was investigated.

2 Experimental

2.1 Instrument and reagents

The instruments used in the present work were similar to the instruments used in the previous work [43]. Norepinephrine, benzoyl ferrocene and the other reagents with analytical grade were purchased from Merck (Darmstadt, Germany). The phosphate buffer solution (PBS) was prepared from concentrate H_3PO_4 and their salts. All solutions were prepared using deionized water. The MF NPs were synthesis according to previous reports [44].

2.2 Preparation of electrode

10 mg BF, 100 mg of MF and 890 mg graphite powder were mixed using a mortar and pestle for 10 min, and then 0.7 mL of paraffin was added to it and remixed for 10 min. Then, the resultant paste inserted into a glass tube (long = 10 cm; i.d. = 3.4 mm) and from the other side a copper wire is inserted to establish the electrical connection. After that, to get a smooth and polished surface, we pressed additional paste out of the glass tube and use a piece of paper to polish it. However, the resulting electrode is displayed with BFMFCPE.

Furthermore, the BFCPE without MF, MF paste electrode (MFCPE) without BF, as well as the bare CPE where there were not MF and BF were constructed for comparison.

2.3 Preparation process of the real samples

Urine samples were transferred to a refrigerator immediately after collection. In the next step, a 0.45 μm filter was used to filter them and then, 10 mL of each sample transferred to a 50.0 mL volumetric balloon and diluted with PBS (pH 3.0). Since there was no NE in the urine sample, an appropriate amount of standard NE was added to the collected urine before centrifugation and filtration. The human serum samples were prepared from a Hospital and ten-fold diluted with PBS (pH 3.0).

2.4 Synthesis of manganese ferrite nanoparticle

The MF NPs were synthesis according to previous reports [44]. For this synthesis, 13.4 g iron nitrate and 4.9 g manganese nitrate were added to 70 mL of aqueous solution containing 3.0 mL ethylene diamine and 4.2 g NaOH. The resulting solution was heated to 85 $^{\circ}\text{C}$ and kept at this temperature for 60 min to complete the reaction. The precipitate was filtered off and placed in an oven at 85 $^{\circ}\text{C}$ for 1 h. In the following, the obtained material was calcined for 60 min in an alumina crucible at 500 $^{\circ}\text{C}$.

3 Results and discussion

3.1 Characterization of MF NPs

The surface morphology of MF NPs was assessed using scanning electron microscope image and shown that MF NPs are relatively uniform and have the spherical morphology (Fig. 1).

The FT-IR analysis data of the MF NPs in a frequency ranging between 400 and 4000 cm^{-1} is given in Fig. 2. The absorption peak around 3450 cm^{-1} could be attributed to the O–H stretching vibration and absorption peak around 500–600 cm^{-1} could be attributed to the O–metal vibration. The band that appears at 1025 cm^{-1} could be attributed to vibration of Si–O–Metal [45]. The peak appeared in around 3435 cm^{-1} could be attributed to the N–H(stretching

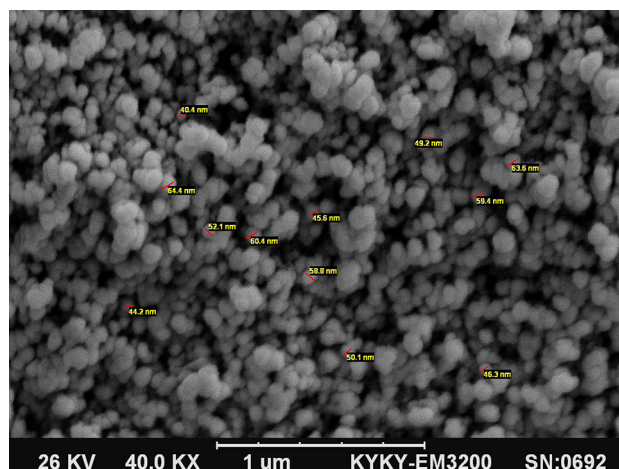


Fig. 1 The SEM picture of MF NPs

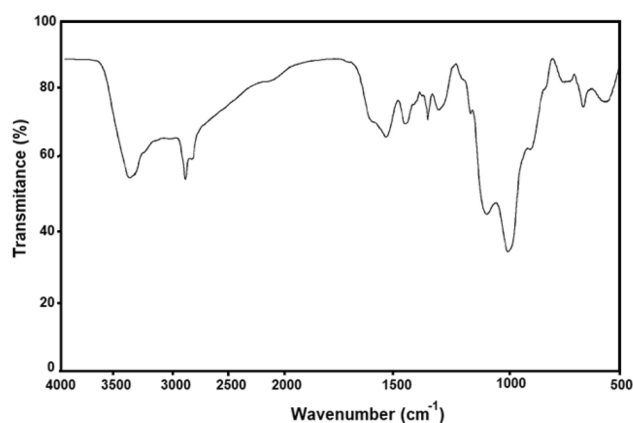


Fig. 2 FT-IR of MF NPs

vibration) and the peak appeared in around 2927 cm^{-1} could be attributed to the $-\text{CH}_2-$ asymmetric vibration. The peak appearing at 2864 cm^{-1} can be due to the $-\text{CH}_2-$ symmetric vibration and the peak appearing at 1560 cm^{-1} can be due to the C–N (amine) bending vibration. Also, the peak appearing at 1120 cm^{-1} can be due to the C–N stretch (aliphatic amine).

The phase identification and crystalline structures of the MF NPs are shown in Fig. 3. The shown diffraction peaks at 30.2 $^{\circ}$, 35.5 $^{\circ}$, 43.2 $^{\circ}$, 53.6 $^{\circ}$, 57.1 $^{\circ}$ and 62.6 $^{\circ}$ belonging to the miller planes (220), (311), (400), (422), (511) and (440) indicate that the nanoparticles synthesized is MF NPs having spinel FCC form and corresponded to values from JCPDS file No.10-0319 [46–48]. The crystalline size was calculated by Scherer Eq. (1).

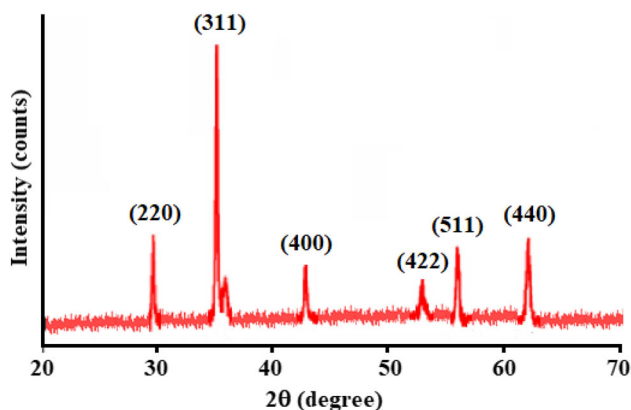


Fig. 3 XRD pattern of the synthesized MF NPs

$$D = \frac{0.9\lambda}{\beta \cos\theta} \quad (1)$$

In this equation, the half maximum of the main diffraction peak (311) is β and the λ is 0.15406 nm [48]. The calculated size of crystallites was in the range of 27.6 nm that confirmed the nanocrystalline structure of the given material.

Figure 4 shows EDX spectra of the MF NPs, and as can be seen existence of Fe, Mn, and O elements with weight ratios of Fe (56.0%), Mn (28.1%) and O (15.9%) was confirmed.

3.2 Characterization of BFMFCPE

The morphology of BFMFCPE electrode was characterized by SEM (Fig. 5) and showed that both materials (BF and MF) are present on the surface of the BFMFCPE. Also, as shown in the Fig. 5, spherical MF nanoparticles with an average diameter of 41 nm are well distributed on the electrode surface.

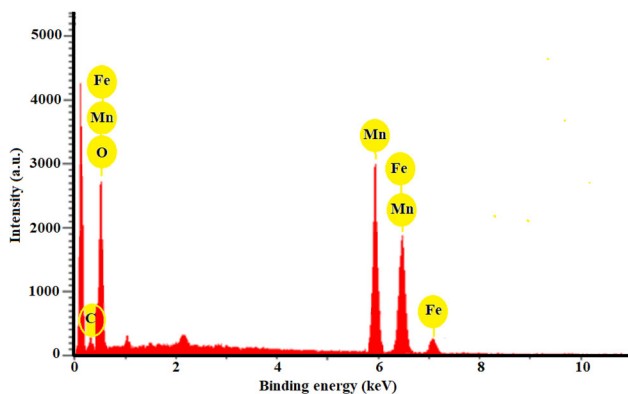


Fig. 4 EDX spectrum of the MF NPs

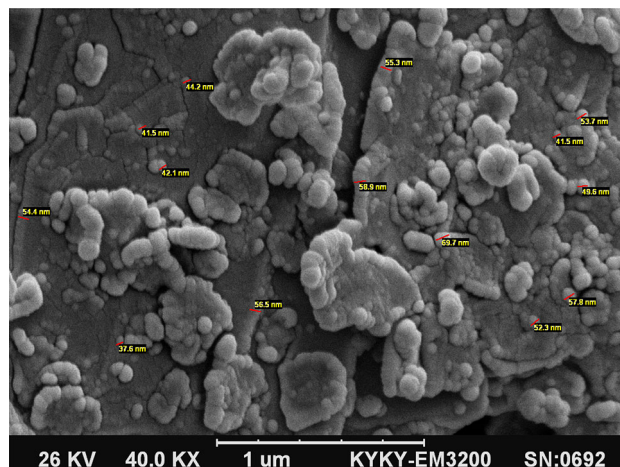


Fig. 5 SEM of BFMFCPE electrode

3.3 Electrochemical behavior of BFMFCPE

The BFMFCPE was initially fabricated and then its electrochemical features were investigated in 0.1 M of PBS (pH 3.0) by CV (Fig. 6). Attained test findings indicated the reproducible anodic and cathodic peaks with E_{pa} , E_{pc} and E^o of 625, 535 and 580 versus Ag/AgCl/KCl (3.0 M), respectively. The calculated peak separation potential, $\Delta E_p = (E_{pa} - E_{pc})$ of 90 mV, was higher than $59/n$ mV, as expected for a reversible system [48], this shows a quasi-reversible behavior of the redox couple of BF in BFMFCPE in aqueous medium.

3.4 Electrochemical impedance spectroscopy studies

Modification of electrode with MF NPs and BF was assessed by electrochemical impedance spectroscopy (EIS) method in a solution containing 0.5 mM

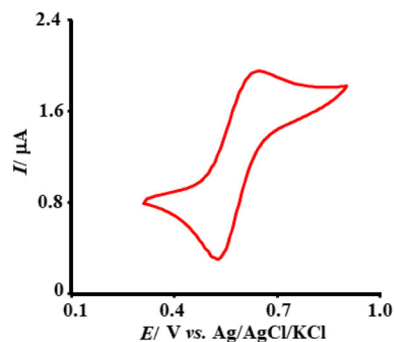


Fig. 6 CV for BFMFCPE in 0.1 M PBS (pH = 3.0) with the scan rate of 50 mVs^{-1}

$[\text{Fe}(\text{CN})_6]^{-3/4-}$ (Fig. 7). As can be seen, the value of charge transfer resistance at the surface of the bare electrode (curve a) is much higher than the modified electrode (curve b). This point confirms highly conductivity of MF NPs at the surface of the electrode.

3.5 Effective surface area of electrodes

In order to illustrate that the MF NPs could increase the electrode surface area in comparison to the surface of unmodified CPE, real surface area of all electrodes was determined by the Randles–Sevcik (Eq. 2) [49]:

$$I = (2.69 \times 10^5) ACD^{1/2}n^{3/2}v^{1/2} \quad (2)$$

In the Eq. 2, “ A ” is the effective surface area of each electrode (cm^2), “ n ” is the number of electrons taking part in charge transfer process, “ D ” is the diffusion coefficient of the analyte in the solution and “ C ” is the concentration of the analyte in the solution. The values of n and D for $\text{K}_3\text{Fe}(\text{CN})_6$ are 1 and $7.6 \times 10^{-6} \text{ cm}^2\text{s}^{-1}$, respectively.

The results showed that the real surface area of CPE, BFCPE, MFCPE and BFMFCPE were 0.09, 0.09, 20.7 and 20.7 cm^2 , respectively. Therefore, as expected, the surface area of MFCPE increases with the addition of MF NPs to the matrix of the carbon paste.

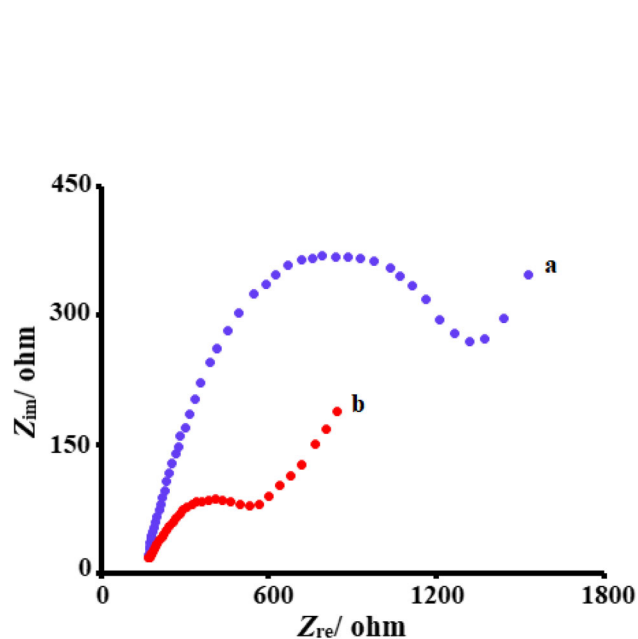


Fig. 7 Nyquist diagrams of bare SPE (a) and BFMFCPE (b) in the presence of 0.5 mM $[\text{Fe}(\text{CN})_6]^{-3/4-}$ pH 3.0

3.6 Electrochemical behaviour of norepinephrine at the BFMFCPE surface

Figure 8 represents CVs for electrochemical oxidation of 120.0 μM NE at the bare CPE (i.e., curve c), MFCPE (i.e., curve d), BFCPE (i.e., curve e), and finally, BFMFCPE (i.e., curve f). Also, the CVs responses for the bare CPE and the BFMFCPE in 0.1 M PBS (pH 3.0) were presented in curve 8a and 8b, respectively.

As can be seen, potential of peak (E_p) for NE is 630 mV and 700 mV at the BFMFCPE surface and the bare CPE, which reflects the capability of BF and MF as good mediators. Compared to the unmodified electrode, the E_p is shifted by about 70 mV to negative values. However, compared to the unmodified electrode, the peak current (I_p) in 120.0 μM NE solution (curve d) considerably elevated, which was caused by the probable electrocatalytic impacts of BFMFCPE on NE.

Based on these results, we propose an EC' catalytic mechanism, shown in scheme 1, to describe the electrooxidation of NE at the surface of BFMFCPE. In this scheme, NE oxidized in the catalytic reaction (C), by the oxidized form of BF produced at the electrode surface via an electrochemical (E) reaction.

On the other hands, the electrochemical behavior of NE is dependent on the pH of the electrolyte solution,

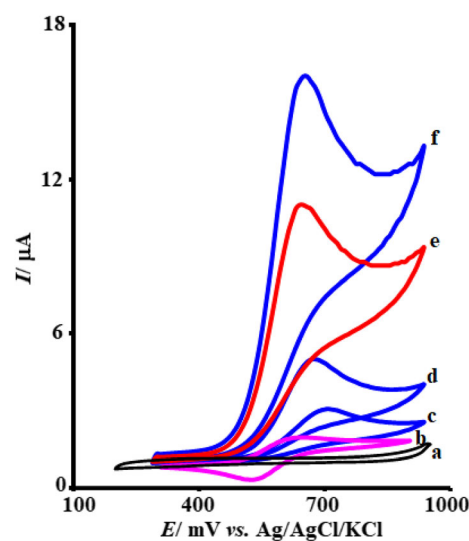
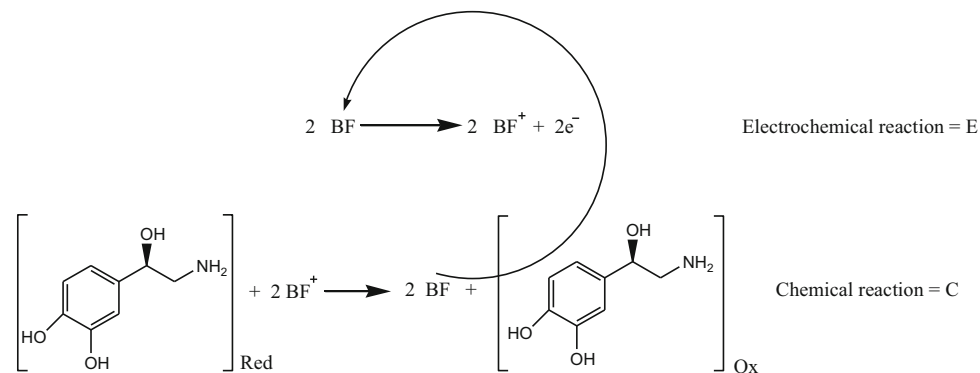


Fig. 8 The CVs of the bare CPE (c), the MFCPE (d), the BFCPE (e) and the BFMFCPE in the presence of 100.0 μM NE into 0.1 M PBS (pH of 3.0); and also, the cyclic voltammograms of the unmodified CPE (a) and the BFMFCPE (b) into 0.1 M PBS (pH of 3.0). Scan rate equaled 50 mV s^{-1} in all cases

Scheme 1 The electrooxidation of NE at the surface of BFMFCPE



while the electrochemical properties of the BF (Ferrocen/Ferrocen⁺ redox couple) is pH-independent. Therefore, investigating the effect of electrolyte solution pH in order to determine the optimal pH is one of the necessities of research. For this reason, the LSV was used to examine the electrochemical behavior of NE at different pHs ($2.0 < \text{pH} < 9.0$) (Fig. 9). Data have shown higher utility of the electrocatalytic oxidation of NE at the BFMFCPE surface at acidic circumstances than the basic or neutral

media (Inset of Fig. 9). Therefore, we chose pH of 3.0 as an optimum pH to oxidize NE at the BFMFCPE surface.

In the following, the effect of scanning speed on the I_p of NE was assessed using LSV (Fig. 10). The observations showed that the higher the scan speed, the higher the I_p and the E_p shifted towards higher positive potentials. As can be seen (Inset of Fig. 10), the I_p vs. the square root of the scanning rate ($v^{1/2}$) varied linearly, therefore, the oxidation process of NE at the BFMFCPE is controlled by diffusion [49].

In the next step, the LSV obtained at the scan rate of 10 mVs^{-1} was used for draw the TOEFL diagram (Fig. 11). The ascending part of the voltammogram is called the TOEFL region that under the influence by

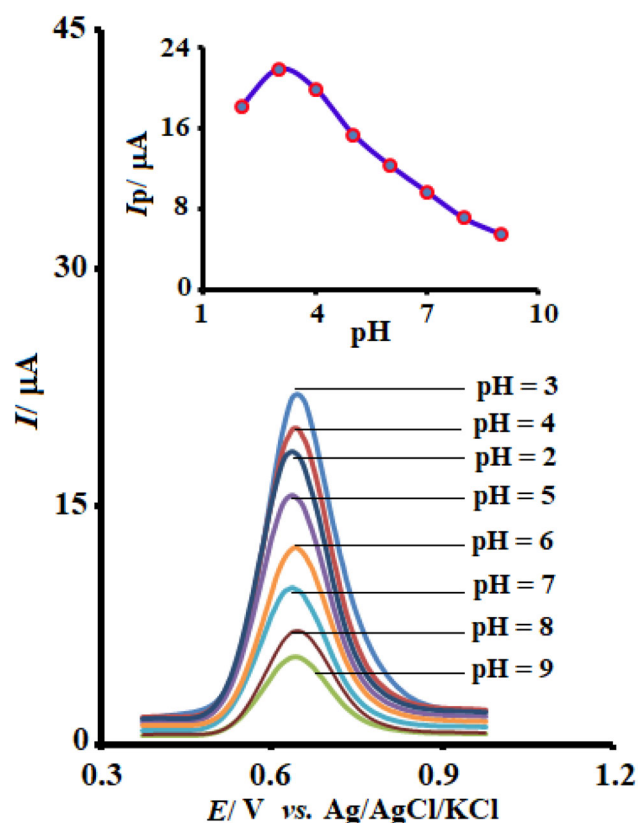


Fig. 9 LSVs of BFMFCPE in 0.1 M PBS with different pH values (2–9) containing $120.0 \mu\text{M}$ NE. Inset: Variation I_p with pH

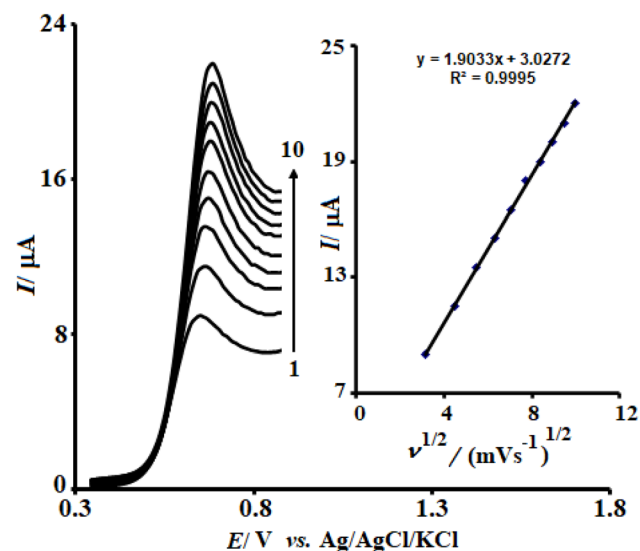


Fig. 10 LSVs of the BFMFCPE into 0.1 M PBS (pH of 3.0) containing $120.0 \mu\text{M}$ NE at different scan rates. 1–10 denoted to 10, 20, 30, 40, 50, 60, 70, 80, 90 and 100 mVs^{-1} . Inset: Variations in the anodic peak current versus the square root of the scan rates

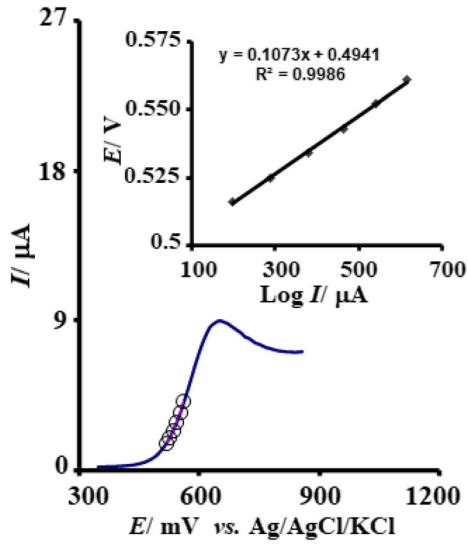


Fig. 11 A Tafel plot extracted from LSV of BFMFCPE into 0.1 M PBS (pH of 3.0) containing 120.0 μM NE at a scan rate equal to 10 mV s⁻¹

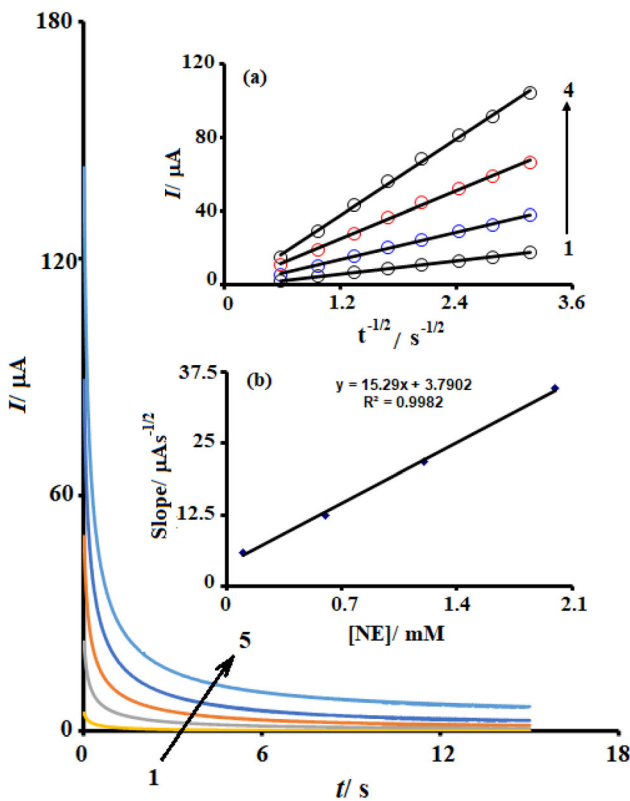


Fig. 12 The obtained chronoamperograms at the BFMFCPE into 0.1 M PBS (pH of 3.0) containing different concentrations of NE. It is notable that 1–5 are corresponding to 0.0, 0.1, 0.4, 0.9 and 1.5 mM of NE. Insets: The plot of I versus $t^{-1/2}$ obtained from the chronoamperograms 1–4 (a), the slope of straight lines against concentration of NE (b)

the electron transfer kinetic between NE and the BFMFCPE.

Due to the slope of the TOEFL curve, which corresponds well to the involvement of 1 electron in the electrode rate-determining step [49], a charge transfer coefficient (α) of 0.45 was obtained for NE. In addition, a charge transfer coefficient ($\alpha = 0.24$) was obtained for NE on the surface of unmodified CPE. As can be seen, the value of α has been improved by modifying the electrode surface.

3.7 Chronoamperometric measurements

In the next step, the chronoamperometry of NE at the surface of BFMFCPE was assessed. For perform of this study, we adjusted the working electrode potential at 0.75 V versus Ag/AgCl/KCl (3.0 M) using diverse concentrations of NE into PBS at a pH of 3.0 (Fig. 12). It should be mentioned that we used Cottrell equation (Eq. 3) to describe the current generated for the electrochemical oxidation of a material under conditions where mass transfer is limited. In this case, the material has a diffusion coefficient that is denoted by D [49]:

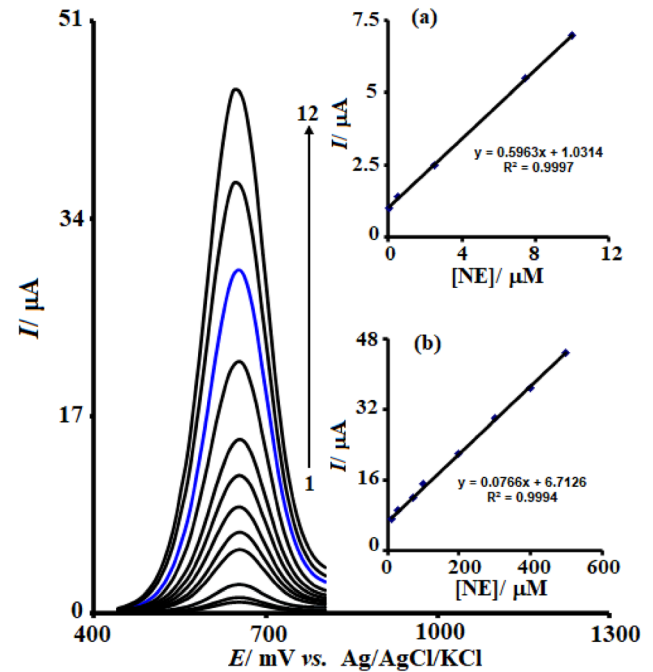


Fig. 13 The DPV of the BFMFCPE into 0.1 M PBS (pH of 3.0) containing different concentrations of NE (0.03, 0.5, 2.5, 7.5, 10.0, 30.0, 70.0, 100.0, 200.0, 300.0, 400.0 and 500.0 μM). Inset: The peak current plots versus concentration of NE in ranges from 0.03–10.0 to 10.0–500.0 μM

Table 1 Comparison of the figure of merit of the BFMFCPE compared to other electrodes used in the measurement of NE

Method	Sensitivity ($\mu\text{A } \mu\text{M}^{-1} \text{ cm}^2$)	LOD (nM)	Dynamic range (μM)	Ref.
Glassy carbon electrode modified with poly(L-arginine)/reduced graphene oxide composite	0.746	42.2	0.8–9 20–70	[2]
Glassy carbon electrode modified with CTAB-SnO ₂ NPs	0.048	6	0.1–1 1–300	[3]
Glassy carbon electrode modified with 2-amino-1,3,4- thiadiazol	0.238	0.17	0.04–25	[8]
ZrO ₂ nanoparticles-modified carbon paste electrode	0.0153	89.5	0.1–2000	[9]
CPE modified with 5-mino-3',4'- dimethyl-biphenyl-2-ol and carbon nanotubes	0.040	0.59	1.2–900	[10]
Glassy carbon electrode modified with Au-nanoparticles/poly(2-Amino-2-hydroxymethyl-propane-1,3-diol) film	0.1024	37.3	1.3–230.1	[11]
Glassy carbon electrode modified with cerium doped hydroxyapatite	0.0339	64	0.1–230	[12]
Ionic liquid/multiwall carbon nanotubes paste electrode	0.0841	90	0.3–30 30–450	[13]
CPE modified with Si-Ti -AuNP	0.096	260	20–180	[14]
CPE modified with carbon nanotubes and a molybdenum (VI) complex	0.3229	0.43	0.008–700	[15]
BFMFCPE	0.5963	20.0	0.03–10 10–500	This work

$$I = nFAD^{1/2}C_b\pi^{-1/2}t^{-1/2}, \quad (3)$$

here C_b and D imply the bulk concentration (mol cm^{-3}) and diffusion coefficient ($\text{cm}^2 \text{ s}^{-1}$). We also applied experimental plots of I versus $t^{-1/2}$, with the best fits for diverse concentrations of NE (Fig. 12a). In the next step, we plotted the slope of the resultant straight lines versus (Fig. 12b) concentration of NE. Using the Cottrell equation and considering the slope of the curve, the average of D for NE was obtained as $2.4 \times 10^{-6} \text{ cm}^2/\text{s}$.

3.8 Repeatability and stability

We used DPV to assess the repeatability of BFMFCPE. The obtained results showed that RSD for ten measurements of $100.0 \mu\text{M}$ NE equaled 3.2%, which demonstrates a reasonable repeatability of sensor. Moreover, stability of BFMFCPE was assessed by storage of modified electrode for 21 days for investigating storage stability of the NE sensor. According to the outputs, the current signal after 21 days was 96.7% of its initial value, which illustrates a high stability. It is necessary to mention, after each measurement, the BFMFCPE was polished.

3.9 Calibration plot and detection limit

Preliminary investigations showed that, the I_p of NE can be used to detect NE in solution. It has been found that DPV benefits from the enhanced sensitivity and more acceptable features for analytical utilizations; therefore, this method was used to investigate the linear range of the BFMFCPE (Fig. 13). For this purpose, the BFMFCPE was placed in a series of NE solutions with different concentrations and peak current was measured. According to the findings, electrocatalytic peak current of the NE oxidation at the BFMFCPE surface has two linear dependence on the NE concentration in ranges from 0.3×10^{-7} – 1.0×10^{-5} to 1.0×10^{-5} – 5.0×10^{-4} M. Detection limit of NE based on 3 s was 20.0 nM (see Table 1).

3.10 Interference effect

In the analytical chemistry, the selectivity of sensor is a very important factor. For this assesses, the effect of some annoying species on the measurement of $100.0 \mu\text{M}$ NE was assessed by DPV under optimum conditions. The possible interfering species were selected in such a way that they could be present either in the pharmaceutical's product or in the biological fluids accompanying the NE. The obtained data (Figs. 14, S1) showed that tenfold KCl, NaCl,

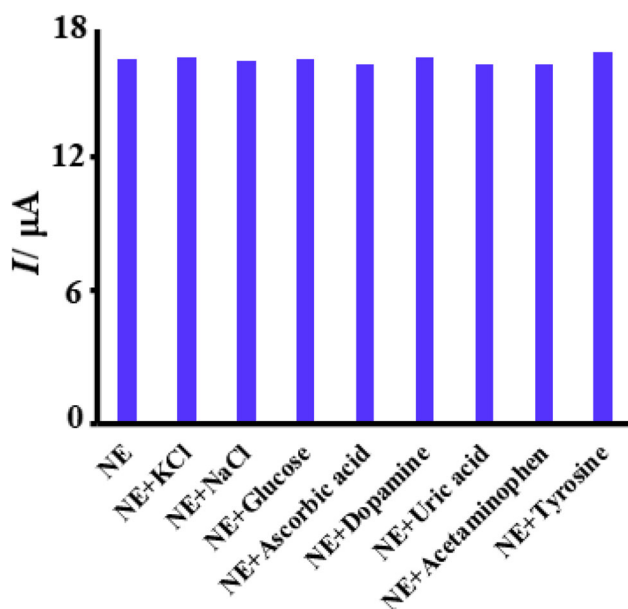


Fig. 14 The I_p of the BFMFCPE to 120 μM of NE, which is 1.2 mM relative to each disturbing species

Table 2 Application of the BFMFCPE to detect NE in the real specimen ($n = 5$)

Sample	Spiked (μM)	Found (μM)	Recovery (%)	RSD (%)
Urine	–	ND*	–	–
	10.0	9.9 ± 0.3	99.0	3.3
	20.0	20.5 ± 0.6	102.5	3.2
	50.0	48.4 ± 1.4	96.8	2.9
Serum	–	ND	–	–
	10.0	10.2 ± 0.3	102.0	3.2
	20.0	19.5 ± 0.5	97.5	2.9
	50.0	51.8 ± 1.6	103.6	2.8

*Not detect

glucose, ascorbic acid, dopamine, uric acid, acetaminophen and tyrosine show no disturbance in the measurement of NE and the change in I_p due to interfere was less than 5%. Therefore, can be said that the electrode has a good selectivity.

3.11 Real-sample analysis

To evaluate the applicability of the BFMFCPE in determining the true samples, the pre-prepared sample was transferred to electrochemical cell and the amount of NE was measured using a DPV. The standard addition method was used to increase the

accuracy of the measurement. The results are given in Table 2 and showed that the recovery percentages are in the range of 96.8–103.6%. Also, the RSD percentages of the method were 3.3% or less, which indicates the high reliability of the BFMFCPE in real samples.

4 Conclusions

In this research, a new modified CPE was constructed for the measurement of NE. Modification of the electrode surface using BF and MF nanocomposite increased the electrode response to NE and thus increased the sensitivity of the measurement. The BFMFCPE was successfully applied for the measurement of NE in urine and serum samples. Simplicity, portability and cost-effectiveness are some of the advantages of the developed BFMFCPE.

Acknowledgements

The author is grateful to Islamic Azad University, Kerman Branch, for financial assistance of this work.

Funding

The authors have not disclosed any funding.

Data availability

The authors confirm that the data supporting the findings of this study are available within the article and its supplementary materials.

Declarations

Conflict of interest The authors declare that they have no competing interests.

Supplementary Information: The online version contains supplementary material available at <http://doi.org/10.1007/s10854-022-08145-5>.

References

1. M. Dai, B. Haselwood, B.D. Vogt, J.T.L. Belle, Amperometric sensing of norepinephrine at picomolar concentrations

- using screen printed, high surface area mesoporous carbon. *Anal. Chim. Acta* **788**, 32 (2013)
- S.K. Anand, M.R. Mathew, J. Radecki, H. Radecki, K.G. Kumar, Individual and simultaneous voltammetric sensing of norepinephrine and tyramine based on poly (Larginine)/reduced graphene oxide composite film modified glassy carbon electrode. *J. Electroanal. Chem.* **878**, 114531 (2020)
 - N. Lavanya, C. Sekar, Electrochemical sensor for simultaneous determination of epinephrine and norepinephrine based on cetyltrimethylammonium bromide assisted SnO₂ nanoparticles. *J. Electroanal. Chem.* **801**, 503–510 (2017)
 - S. Sheikh, S.E. Haque, S.S. Mir, Neurodegenerative diseases: multifactorial conformational diseases and their therapeutic interventions. *Am. J. Neurodegener. Dis.* **8**, 563481 (2013)
 - M.M. Ardakani, M.A.S. Mohseni, M.A. Alibeik, A. Benvidi, Electrochemical sensor for simultaneous determination of norepinephrine, paracetamol and folic acid by a nanostructured mesoporous material. *Sens. Actuators B Chem* **380**, 171 (2012)
 - C.R. Lake, B. Chernow, D.S. Goldstein, D.G. Glass, M. Coleman, M.G. Ziegler, Plasma catecholamine levels in normal subjects and in patients with secondary hypertension. *Fed. Proc.* **43**, 52–56 (1984)
 - V. Carrera, E. Sabater, E. Vilanova, M.A. Sogorb, A simple and rapid HPLC–MS method for the simultaneous determination of epinephrine, norepinephrine, dopamine and 5-hydroxytryptamine: application to the secretion of bovine chromaffin cell cultures. *J. Chromatogr. B* **847**, 88–94 (2007)
 - P. Kalimuthu, S.A. John, Selective determination of norepinephrine in the presence of ascorbic and uric acids using an ultrathin polymer film modified electrode. *Electrochim. Acta* **56**, 2428–2432 (2011)
 - M. Mazloum-Ardakani, H. Beitollahi, M.K. Amini, F. Mirkhalaf, M. Abdollahi-Alibeik, New strategy for simultaneous and selective voltammetric determination of norepinephrine, acetaminophen and folic acid using ZrO₂ nanoparticles-modified carbon paste electrode. *Sens. Actuators B* **151**, 243–249 (2010)
 - H. Beitollahi, S. Mohammadi, Selective voltammetric determination of norepinephrine in the presence of acetaminophen and tryptophan on the surface of a modified carbon nanotube paste electrode. *Mater. Sci. Eng. C* **33**, 3214–3219 (2013)
 - M. Taei, G. Ramazani, Simultaneous determination of norepinephrine, acetaminophen and tyrosine by differential pulse voltammetry using Au-nanoparticles/poly(2-Amino-2-hydroxymethylpropane-1,3-diol) film modified glassy carbon electrode. *Coll. Surf. B* **123**, 23–32 (2014)
 - P. Kanchana, M. Navaneethan, C. Sekar, Fabrication of Ce doped hydroxyapatite nanoparticles based non-enzymatic electrochemical sensor for the simultaneous determination of norepinephrine, uric acid and tyrosine. *Mater. Sci. Eng. B* **226**, 132–140 (2017)
 - S. Salmanpour, T. Tavana, A. Pahlavan, M.A. Khalilzadeh, A.A. Ensafi, H. Karimi-Maleh, H. Beitollahi, E. Kowsari, D. Zareyee, Voltammetric determination of norepinephrine in the presence of acetaminophen using a novel ionic liquid/multi-wall carbon nanotubes paste electrode. *Mater. Sci. Eng. C* **32**, 1912–1918 (2012)
 - F.M. Morawski, B.B. Xavier, A.H. Virgili, K.S. Caetano, E.W. Menezes, E.V. Benvenuti, T.M. Haas Costa, L.T. Arenas, A novel electrochemical platform based on mesoporous silica/titania and gold nanoparticles for simultaneous determination of norepinephrine and dopamine. *Mater. Sci. Eng. C* **120**, 111646 (2021)
 - H. Beitollahi, I. Sheikhshoae, Selective voltammetric determination of norepinephrine in the presence of acetaminophen and folic acid at a modified carbon nanotube paste electrode. *J. Electroanal. Chem.* **661**, 336–342 (2011)
 - S. Huang, P.F. Wu, H.Y. Yue, X. Gao, S.S. Song, X.R. Guo, H.T. Chen, ZnO nanosheet arrays/graphene foam: voltammetric determination of dopamine in the presence of ascorbic acid and uric acid. *J. Mater. Sci. Mater. Electron.* **30**, 16510–16517 (2019)
 - S. Boobphahom, T. Siripongprea, D.D. Zhang, J. Qin, P. Rattanawaleedirojn, N. Rodthongkum, TiO₂/MXene-PVA/GO hydrogel-based electrochemical sensor for neurological disorder screening via urinary norepinephrine detection. *Microchim. Acta* (2021). <https://doi.org/10.1007/s00604-021-04945-4>
 - R.N. Goyal, S. Bishnoi, Simultaneous determination of epinephrine and norepinephrine in human blood plasma and urine samples using nanotubes modified edge plane pyrolytic graphite electrode. *Talanta* **84**, 78–83 (2011)
 - P.S. Doshi, D.J. Edwards, Effects of L-dopa on dopamine and norepinephrine concentrations in rat brain assessed by gas chromatography. *J. Chromatogr. A* **210**, 505–511 (1981)
 - C.L. Guan, J. Quyang, Q.L. Li, B.H. Liu, W.R.G. Baeyens, Simultaneous determination of catecholamines by ion chromatography with direct conductivity detection. *Talanta* **50**, 1197–1203 (2000)
 - F.B. Salem, Spectrophotometric and titrimetric determination of catecholamines. *Talanta* **34**, 810–812 (1987)
 - T.A. Esquivel-Castro, M.C. Ibarra-Alonso, J. Oliva, A. Martínez-Luévanos, Porous aerogel and core/shell nanoparticles for controlled drug delivery: a review. *Mater. Sci. Eng. C* **96**, 915–940 (2019)
 - P. Sehrawat, R.K. Malik, R. Punia, M. Sheoran, N. Kumari, S.P. Khatkar, V.B. Taxak, Luminescence tuning and structural analysis of new BaYAlZn₃O₇:Sm³⁺ nanomaterials with

- excellent performance for advanced optoelectronic appliances. *J. Mater. Sci.* **32**, 15930–15943 (2021)
24. A.F. Moreira, C.F. Rodrigues, C.A. Reisa, E.C. Costa, I.J. Correia, Gold-core silica shell nanoparticles application in imaging and therapy: a review. *Micropor. Mesopor. Mater.* **270**, 168–179 (2018)
 25. S.Z. Mohammadi, H. Beitollahi, M. Kaykhahi, N. Mohammadzadeh, S. Tajik, R. Hosseinzadeh, Simultaneous determination of droxidopa and carbidopa by carbon paste electrode functionalized with NiFe₂O₄ nanoparticle and 2-(4-ferrocenyl-[1,2,3] triazol-1-yl)-1-(naphthalen-2-yl) ethenone. *Measurement* **155**, 107522 (2020)
 26. H. Liang, Y. Zhao, H. Ye, C.-P. Li, Ultrasensitive and ultra-wide range electrochemical determination of bisphenol A based on PtPd bimetallic nanoparticles and cationic pillar[5] arene decorated graphene. *J. Electroanal. Chem.* **855**, 113487 (2019)
 27. H. Beitollahi, F. Movahedifar, S. Tajik, Sh. Jahani, A review on the effects of introducing CNTs in the modification process of electrochemical sensors. *Electroanalysis* **31**, 1195–1203 (2019)
 28. Y. Ran, Y. Li, X. Cui, T. Lai, L. Yao, R. Zhao, L. Wang, Y. Wang, Sm-doped SnO₂ nanoparticles synthesized via solvothermal method as a high-performance formaldehyde sensing material for gas sensors. *J. Mater. Sci. Mater. Electron.* **32**, 8249–8264 (2021)
 29. S.Z. Mohammadi, H. Beitollahi, Z. Dehghan, R. Hosseinzadeh, Electrochemical determination of ascorbic acid, uric acid and folic acid using carbon paste electrode modified with novel synthesized ferrocene derivative and core-shell magnetic nanoparticles in aqueous media. *Appl. Organometal. Chem.* **32**, 4551 (2018)
 30. H.-A. Kalaleh, K. Masri, The role of butanol isomers on the performance of ammonia sensors based on polypyrrole prepared by microemulsion polymerization. *J. Mater. Sci. Mater. Electron.* **32**, 8978–8988 (2021)
 31. H. Beitollahi, M.A. Khalilzadeh, S. Tajik, M. Safaei, K. Zhang, H.W. Jang, M. Shokouhimehr, Recent advances in applications of voltammetric sensors modified with ferrocene and its derivatives. *ACS Omega* **5**, 2049–2059 (2020)
 32. S. Tajik, Z. Dourandish, K. Zhang, H. Beitollahi, Q.V. Le, H.W. Jang, M. Shokouhimehr, Carbon and graphene quantum dots: a review on syntheses, characterization, biological and sensing applications for neurotransmitter determination. *RSC Adv.* **10**, 15406–15429 (2020)
 33. S. Fan, L. Ji, G. Mao, X. Sui, H. Wang, Y. Zhu, H. Song, Voltammetric determination of phentolamine mesylate in pharmaceutical formulations at poly (4-aminobenzene sulfonic acid)-modified glassy carbon electrode. *Chem. Pap.* **74**, 4411–4417 (2020)
 34. S.Z. Mohammadi, H. Beitollahi, E. Bani Asadi, Electrochemical determination of hydrazine using a ZrO₂ nanoparticles-modified carbon paste electrode. *Environ. Monit. Assess.* **187**, 122 (2015)
 35. C.M. Kuskur, B.E. Kumara Swamy, H. Jayadevappa, P.S. Ganesh, Poly (rhodamine B) sensor for norepinephrine and paracetamol: a voltammetric study. *Ionics* **24**, 3631–3640 (2018)
 36. S. Tajik, H. Beitollahi, P. Biparva, Methyl dopa electrochemical sensor based on a glassy carbon electrode modified with Cu/TiO₂ nanocomposite. *J. Serb. Chem. Soc.* **83**, 863–874 (2018)
 37. A. Yousefi, A. Bagheri, A new sensor based on glassy carbon electrode modified with Fe₃O₄@MCM-48-SO₃H/multi-wall carbon nanotubes composite for simultaneous determination of norepinephrine and tyrosine in the presence of ascorbic acid. *Ionics* **25**, 2845–2856 (2019)
 38. S. Esfandiari Baghbamidi, H. Beitollahi, S. Tajik, R. Hosseinzadeh, Voltammetric sensor based on 1-benzyl-4-ferrocenyl-1H-[1,2,3]-triazole/carbon nanotube modified glassy carbon electrode; detection of hydrochlorothiazide in the presence of propranolol. *Int. J. Electrochem. Sci.* **11**, 10874–10883 (2016)
 39. S. Tajik, H. Beitollahi, F. Garkani Nejad, K.O. Kirlikovali, Q.V. Le, H.W. Jang, R.S. Varma, O.K. Farha, M. Shokouhimehr, Recent electrochemical applications of metal-organic framework-based materials. *Cryst. Growth Des.* **20**, 7034–7064 (2020)
 40. S. Kandula, P. Jeevanandam, A facile synthetic approach for SiO₂@Co₃O₄ core-shell nanorattles with enhanced peroxidase-like activity. *RSC Adv.* **5**, 5295–5306 (2015)
 41. W.P. Wicaksono, G.T.M. Kadja, D. Amalia, L. Uyun, W.P. Rini, A. Hidayat, R.L. Fahmi, D. Nasriyanti, S.G.V. Leun, H.A. Ariyanta, T.A. Ivandini, A green synthesis of gold-palladium core-shell nanoparticles using orange peel extract through two-step reduction method and its formaldehyde colorimetric sensing performance. *Nano-Struct. Nano-Objects* **24**, 100535 (2020)
 42. A.A. Ansari, M. Alam, Electrochemical sensitive detection of hydrazine through cobalt-doped cerium oxide nanostructured platform. *J. Mater. Sci. Mater. Electron.* **32**, 13897–13905 (2021)
 43. M. Nazari, H. Asadollahzadeh, M. Shahidi, N. Rastakhiz, S.Z. Mohammadi, An electrochemical nano-sensors for determination of hydrazine using modified electrode by La₂O₃-Co₃O₄ nanohydrates and ionic liquid. *J. Mater. Sci. Mater. Electron.* **32**, 25258–25268 (2021)
 44. S.Z. Mohammadi, A. Seyedi, Preconcentration of cadmium and copper ions on magnetic core-shell nanoparticles for

- determination by flame atomic absorption. *Environ. Toxicol. Chem.* **98**, 705 (2015)
45. Z.Y. Yuan, S.Q. Liu, T.H. Chen, J.Z. Wang, H.X. Li, Synthesis of iron-containing MCM-41. *J. Chem. Soc. Chem. Commun.* **9**, 973–974 (1995)
46. D. Deivatamil, M. John Abel, P. Nancy Dyana, R. Thiruneelakandan, J. Joseph Prince, A comparative study on pure and cobalt doped manganese ferrite (Co: MnFe₂O₄) nanoparticles in their optical, structural, and gas sensing properties. *Solid State Commun.* **339**, 114500 (2021)
47. B. Sahoo, S.K. Sahu, S. Nayak, D. Dhara, P. Pramanik, Fabrication of magnetic mesoporous manganese ferrite nanocomposites as efficient catalyst for degradation of dye pollutants. *Catal. Sci. Technol.* **2**, 1367–1374 (2012)
48. M.A. Yousuf, M.M. Baig, N.F. Al-Khalli, M.A. Khan, M.F. Aly Aboud, I. Shakir, M.F. Warsi, The impact of yttrium cations (Y³⁺) on structural, spectral and dielectric properties of spinel manganese ferrite nanoparticles. *Ceram. Int.* **45**, 10936–10942 (2019)
49. A.J. Bard, L.R. Faulkner, *Electrochemical methods: fundamentals and applications*, 2nd edn. (Wiley, New York, 2001), pp. 100–137

Publisher's Note Springer Nature remains neutral with regard to jurisdictional claims in published maps and institutional affiliations.